



**Application and  
analysis of  
debris-flow early  
warning system in  
Wenchuan**

D. L. Liu et al.

**Application and analysis of debris-flow  
early warning system in Wenchuan  
earthquake-affected area**

D. L. Liu<sup>1</sup>, S. J. Zhang<sup>2,3</sup>, H. J. Yang<sup>3</sup>, Y. H. Jiang<sup>3</sup>, and X. P. Leng<sup>4</sup>

<sup>1</sup>College of Software Engineering, Chengdu University of Information and Technology, Chengdu, China

<sup>2</sup>Key Laboratory of Mountain Hazards and Earth Surface Process, Chinese Academy of Sciences, Chengdu, China

<sup>3</sup>Institute of Mountain Hazards and Environment, Chinese Academy of Sciences, Chengdu, China

<sup>4</sup>College of Information Science and Technology, Chengdu University of Technology, Chengdu, China

Received: 29 July 2015 – Accepted: 4 September 2015 – Published: 30 September 2015

Correspondence to: S. J. Zhang (sj-zhang@imde.ac.cn)

Published by Copernicus Publications on behalf of the European Geosciences Union.

[Title Page](#)

[Abstract](#)

[Introduction](#)

[Conclusions](#)

[References](#)

[Tables](#)

[Figures](#)

[⏪](#)

[⏩](#)

[◀](#)

[▶](#)

[Back](#)

[Close](#)

[Full Screen / Esc](#)

[Printer-friendly Version](#)

[Interactive Discussion](#)



## Abstract

The activities of debris flow (DF) in the Wenchuan earthquake-affected area significantly increased after the earthquake on 12 May 2008. The safety of local people's lives and property has been and will continue to be threatened by DFs in a long term. To this end a physics-based early warning system (EWS) for DF forecasting was developed and applied in this earthquake area. This paper introduces an application of the system in the Wenchuan earthquake-affected area and analyzes the prediction results in comparison to the DF events triggered by the strong rainfall events reported by the local government. The prediction accuracy and efficiency was first compared with contribution-factors-based system currently adopted by the Weather Bureau of Sichuan Province using the storm on 17 August 2012 as a case study. The comparison shows that the failure prediction rate and false prediction rate of the new system is respectively 19 and 21 % lower than the system based on the contribution factors. Consequently, the prediction accuracy is obviously higher than the system based on the contribution factors with a higher operational efficiency. As invited by the Weather Bureau of Sichuan Province, authors have upgraded their prediction system of DF by using this new system before the monsoon of Wenchuan earthquake-affected area in 2013. Two prediction cases on 9 July of 2013 and 10 July of 2014 were chosen here to further demonstrate that the new EWS has a high stability, efficiency and prediction accuracy.

## 1 Introduction

Massive potential instable slopes were left after the Wenchuan earthquake on 12 May 2008 (Zhang et al., 2015), which can be readily transformed into landslides by intensive rainfall and then supply abundant loose solid material for debris flow (DF) formation. The increasing availability of solid material enhanced the activity of DFs, especially in the earthquake-affected area. The enhanced DFs will last 20 to 30 years,

## Application and analysis of debris-flow early warning system in Wenchuan

D. L. Liu et al.

[Title Page](#)

[Abstract](#)

[Introduction](#)

[Conclusions](#)

[References](#)

[Tables](#)

[Figures](#)

[⏪](#)

[⏩](#)

[◀](#)

[▶](#)

[Back](#)

[Close](#)

[Full Screen / Esc](#)

[Printer-friendly Version](#)

[Interactive Discussion](#)



## Application and analysis of debris-flow early warning system in Wenchuan

D. L. Liu et al.

[Title Page](#)

[Abstract](#)

[Introduction](#)

[Conclusions](#)

[References](#)

[Tables](#)

[Figures](#)

[⏪](#)

[⏩](#)

[◀](#)

[▶](#)

[Back](#)

[Close](#)

[Full Screen / Esc](#)

[Printer-friendly Version](#)

[Interactive Discussion](#)

and they will threaten lives and properties of local residents for a long time (Tang et al., 2009; Xie et al., 2009). The construction of DF control works is an effective mode for DF defense. However, there are so many DF valleys in need of disaster mitigation and the construction of DF control works will cost a great deal of money and take a long time (Papa et al., 2013). Therefore, building an early warning system (EWS) to predict DF within the Wenchuan earthquake-affected area is deemed an essential choice for disaster mitigation.

All disasters such as floods, landslides, collapses, and DFs can be predicted using EWS, but the EWS in this study will only focus on the function of DF prediction just like the specific EWS for landslide prediction in Hong Kong (Chen and Lee, 2004). EWS has become essential feature of Civil Protections and is commonly recognized as vital risk prevention tools (European Commission DG Environment, 2008). In recent years, there has been a tendency towards increasing the number of operational landslide and DF EWS (Berenguer et al., 2015). For example, the EWS used for predicting DF and landslides in Japan (Osanai et al., 2010), and the landslides EWS in Hong Kong (Chen and Lee, 2004), as well as some regional systems for DF prediction in China (Wei et al., 2007) and in Italy (Aleotti, 2004). All the mentioned EWS are based on the empirical rainfall thresholds derived from the analysis of past rainfall events inducing DF. Since the pioneering work by Caine (1980), empirical rainfall thresholds for shallow landslides and DFs have been developed at local, regional and global scales (Giannecchini et al., 2012; Borga et al., 2014; Vennari et al., 2014). But in fact, rainfall thresholds can only be obtained from the DF valleys where certain amounts of rainfall and related DF data are available (Papa et al., 2013; Zhang et al., 2014b), so these values are difficult to determine in any valley or region. Additionally, Guzzetti et al. (2007, 2008) pointed that most of empirical rainfall thresholds available in literature were defined using non objective and poorly reproducible methods (Gariano et al., 2015). Anyway, the mentioned problems of identifying empirical rainfall thresholds are mainly attributed to a lack of physical framework of DF formation, and hence the accuracy of the EWS based on this empirical mode is relatively low (Wei et al., 2004). For example, a false alarm rate

## Application and analysis of debris-flow early warning system in Wenchuan

D. L. Liu et al.

[Title Page](#)

[Abstract](#)

[Introduction](#)

[Conclusions](#)

[References](#)

[Tables](#)

[Figures](#)

[⏪](#)

[⏩](#)

[◀](#)

[▶](#)

[Back](#)

[Close](#)

[Full Screen / Esc](#)

[Printer-friendly Version](#)

[Interactive Discussion](#)



around 40% is reported for threshold relationships in Alpine region (Badoux et al., 2012). So a physics-based EWS that accounts for the formation mechanism of DF is deemed a path to solving these issues (Zhang et al., 2014a; Papa et al., 2013).

DF initiate when masses of poorly sorted sediment, agitated and saturated with water, sure down slopes, and eventually transform back into nearly rigid deposits (Iverson et al., 1997). This description focused on landslide-induced DF transforming from a single slope when it contains or acquires sufficient water for saturation. Scholars have established some prediction models based on this initiation type of DF using several key hydrological factors such as soil water content, pore water pressure (Cui, 1991; Iverson et al., 1997). But attributing to localized space scale (single slope), these prediction models cannot allow users to conclude whether there is a DF formation at a watershed scale, because DF formation in this larger scale is more complicated (Zhang et al., 2014b).

As for rainfall-induced DF at a watershed scale, there are two dominant types including landslides-inducing (multiple rainfall-induced landslides within a watershed dominate the supplements of solid material for DF formation) and runoff-inducing (sediments of channel bed dominate the supplements of solid material) types (Papa et al., 2013), the former type that mainly distributes within southwest China (Kang, 1987) is our focusing point in this study. In the case of the former type, inadequate material supplements from landslides cannot yield DFs even during extreme rainfall in a DF watershed. The volume of expected point source landslides are keys in understanding the timing and volume forecasting for DFs (Borga et al., 2014). Papa et al. (2013) also argued that the total rainfall-induced landslides are the key factor to DF formation in a watershed, and he used a variable that referred to as failure percentages of landslides to correspond to I-D curves. Using the curve and forecasted rainfall data, DF at a watershed then can be predicted. This pioneering work can derive an I-D curve from a certain amounts of physical numerical simulations no matter whether adequate observation data are available in a watershed, as a consequence, it overcomes the drawback of empirical mode that has to depend on a large number of rainfall and DF data. But the

Papa's model can be only referred as to a quasi-physically based method, because it attempted to predict DF in a watershed without accounting the effect of rainfall-induced runoff.

In fact, rainfall-induced landslides and rainfall (or rainfall-induced runoff) are the two necessary factors for DF formation, the interaction process between them can induce DF formation at a watershed scale (Cui et al., 2013). Hence one can see that the descriptions of DF formation at a watershed scale can be divided into two interaction or coupling process including the first coupling stage between rainfall and slopes leading to soil-mass failure, and the second coupling stage between rainfall-induced runoff and solid material from landslides leading to DF formation (Zhang et al., 2014b).

According to descriptions of the two main coupling processes, the authors developed a prediction model for any DF watershed as long as it is identified as the soil-mechanical DF valley. In this model, the stabilities of slopes within a watershed under the action of rainfall and meanwhile the total volume of rainfall-induced debris deposits from landslides and runoff is simulated at each forecasting step in the first stage, in the second simulating stage, the density of soil–water mixture calculated by the volume of instable soil mass and runoff is constantly simulated at the end of each forecasting step. Using the density of soil–water mixture as the key index, the formation probability of DF at a watershed scale will be identified in time. This model has been performed in different space scale (Jiangjia valley in Yunnan province, China; Sichuan province, China) in order to verify its precision and applicability; the forecasting results are outstanding with low failure-prediction and false-prediction rate (Zhang et al., 2014a, b).

Based on this forecasting model, the main objective of this work is to develop a EWS for DF forecasting that accounts the formation mechanism of DF at a watershed scale, and to introduce the operational effect of this EWS in the Weather Bureau of Sichuan Province. This paper is designed as follows: Sect. 2 describes the study region. Section 3 briefly introduces the basic theory of the forecasting model and describes the working process of the EWS for DF forecasting. Section 4 uses rainfall and related DF event data to verify the accuracy and operational stability of this EWS, and gives a de-

## Application and analysis of debris-flow early warning system in Wenchuan

D. L. Liu et al.

[Title Page](#)

[Abstract](#)

[Introduction](#)

[Conclusions](#)

[References](#)

[Tables](#)

[Figures](#)

[⏪](#)

[⏩](#)

[◀](#)

[▶](#)

[Back](#)

[Close](#)

[Full Screen / Esc](#)

[Printer-friendly Version](#)

[Interactive Discussion](#)

tailed comparison to the forecasting results from the former EWS used in the Weather Bureau of Sichuan Province. Section 5 introduces the operational effect in the Weather Bureau, and discussion and conclusions are summarized in Sect. 6.

## 2 Wenchuan earthquake-affected region

As shown in Fig. 1a, the 2008 Wenchuan earthquake-affected area (IX–XI intensity), with a total area 40 1627 km<sup>2</sup>, is located in the Longmen Shan Mountains of the north-western Sichuan Basin. In this study, the earthquake-affected area within Sichuan Province, shown in Fig. 1b, is selected as the study area. The geological background, topographic setting and climate characteristics of this region provide advantageous conditions for the development and formation of DFs. Frequent mountain hazards (e.g. DFs and landslides) have continuously brought serious damage to this region throughout history (Xie et al., 2009). Before the Wenchuan earthquake, there were 320 DF watersheds identified through field observation (Zhong et al., 1997). Following the Wenchuan earthquake, the DF watersheds increased to 669, according to the data from the Land and Resources Department of Sichuan Province.

### 2.1 Topographic setting

The eastern part of the earthquake-affected area is adjacent to the Sichuan Basin in the east, and the other areas (i.e. the northwest, southwest and northeast) are adjacent to towering mountains. The terrain variations within this region are large, with the elevations ranging from 500 to 5000 m. In general, the western terrain within the region is higher than the eastern. In addition, numerous deep canyons created by large rivers (e.g. the Jialing River, the Fujiang River and the Minjiang River) are common in this region, and their huge elevation differences and large slope gradients can provide the energy conditions necessary for DF formation. The elevations and the slope gradients of the earthquake-affected region are shown in Fig. 2.

## Application and analysis of debris-flow early warning system in Wenchuan

D. L. Liu et al.

[Title Page](#)

[Abstract](#)

[Introduction](#)

[Conclusions](#)

[References](#)

[Tables](#)

[Figures](#)

[⏪](#)

[⏩](#)

[◀](#)

[▶](#)

[Back](#)

[Close](#)

[Full Screen / Esc](#)

[Printer-friendly Version](#)

[Interactive Discussion](#)



## 2.2 Geologic structure

As the main geological structure of the earthquake-affected region, the Longmen Shan fault zone consists of three fault zones, including the Wenchuan–Maoxian fault, the Yingxiu–Beichuan fault and the Peng–Guan fault. Due to its large scale, long geological development and frequent activity, the Longmen Shan fault zone has provided abundant loose solid material (Xie et al., 2009). Additionally, the dramatically increased quantity of loose solid material from the Wenchuan earthquake-induced geological disasters (e.g. collapses, rockfalls and landslides) further enhanced the development conditions of DFs (Wei et al., 2012).

## 2.3 Climate setting

Due to the blocking action of the Longmen Shan Mountains, the warm and wet air from the southeast makes the piedmont region one of the rainstorm centers of north-western Sichuan Province, whereas the leeward slopes to the west are dry. Although the mean annual precipitation in the north of Wenchuan, Maoxian and Lixian counties is 500–800 mm, the maximum daily precipitation can still reach to 35–75 mm. The mean annual precipitation in the south of Wenchuan, Qingchuan and Pingwu counties is 800–1200 mm. The mean annual precipitation of the other regions (e.g. Beichuan, Anxian, Shifang, Mianzhu and Dujiangyan) is greater than 1200 mm, sometimes even reaching 2500 mm (Xie et al., 2009). The runoff caused by rainfall is not only the water component of DFs but also provides the power for DF formation.

## 3 Debris-flow prediction system based on water–soil coupling mechanism

### 3.1 Prediction mechanism of the system

The two soil–water coupling processes described above are the main simulating works in our prediction system. The detailed descriptions are listed in published references

## Application and analysis of debris-flow early warning system in Wenchuan

D. L. Liu et al.

[Title Page](#)

[Abstract](#)

[Introduction](#)

[Conclusions](#)

[References](#)

[Tables](#)

[Figures](#)

[⏪](#)

[⏩](#)

[◀](#)

[▶](#)

[Back](#)

[Close](#)

[Full Screen / Esc](#)

[Printer-friendly Version](#)

[Interactive Discussion](#)





## Application and analysis of debris-flow early warning system in Wenchuan

D. L. Liu et al.

[Title Page](#)

[Abstract](#)

[Introduction](#)

[Conclusions](#)

[References](#)

[Tables](#)

[Figures](#)

[⏪](#)

[⏩](#)

[◀](#)

[▶](#)

[Back](#)

[Close](#)

[Full Screen / Esc](#)

[Printer-friendly Version](#)

[Interactive Discussion](#)

3. Estimation of the probability of DF formation based on the mixture density. The simulations and experiments in the Jiangjia valley (Zhang et al., 2014a) indicate that there is a qualitative relationship between the DF density and the formation probability of DFs. When the value of the mixture density is higher, the formation probability of DFs is larger. According to the research of Kang, the density of the DFs in nature varies in the range of 1.1–2.3 gcm<sup>-3</sup> (Kang et al., 2004). If the DF density in nature is divided into 5 reference intervals, the formation probabilities and warning levels of DFs can be estimated according to the reference intervals listed in Table 1.

### 3.2 Prediction process of the system

The work process of the DF prediction system based on the water–soil coupling mechanism consists of six steps (Fig. 4): basic data preparation, dynamic data inputs, potential DF watershed identification, hydrological process simulation, water–soil mixture density calculation and estimation of DF formation probability. The core parts of this system are the hydrological process simulation and the calculation of the mixture density, and their objects are the potential DF watersheds. In every prediction process, the soil water content value is first updated and saved in the form of disk files from 1 January of the prediction year to the prediction time. The value of the soil water content just before the prediction time is used as the initial value for the following DF prediction. However, this prediction process takes a long time and cannot satisfy the service requirement of DF prediction. To improve the prediction efficiency, the system should be run once to save the value of the soil water content in disk files prior to the rainy season.

1. Acquiring dynamic data. The dynamic data (meteorological data and predicted precipitation data) are provided by the local bureau of meteorology. The meteorological data (e.g. measured rainfall, temperature, relative humidity, wind velocity and sunshine duration) for system should be in raster format with the same range

## Application and analysis of debris-flow early warning system in Wenchuan

D. L. Liu et al.

[Title Page](#)

[Abstract](#)

[Introduction](#)

[Conclusions](#)

[References](#)

[Tables](#)

[Figures](#)

[⏪](#)

[⏩](#)

[◀](#)

[▶](#)

[Back](#)

[Close](#)

[Full Screen / Esc](#)

[Printer-friendly Version](#)

[Interactive Discussion](#)



and resolution as the prediction regional DEM. The data can be obtained by using the spatial interpolation method to handle the data supplied by weather stations. The predicted precipitation data shares the same format, range and resolution with the meteorological data, which can be obtained by using data extraction and resampling techniques to handle the data from Doppler radar.

2. Identification of potential DF watersheds. The system uses the DF watersheds as the prediction units and estimates the formation probability of DFs at the watershed scale. Therefore, it is the principal premise to determine that watersheds in the prediction region have the possibility of DF occurrences. According to Wei's research, the areas of DF watersheds vary from 1 to 100 km<sup>2</sup>, and more than 80 % of DF watershed areas are less than 10 km<sup>2</sup> (Wei et al., 2008). The small watersheds in the prediction region can be extracted by GIS technique, but not all of them are DF watersheds. At present, there are two methods to identify whether a small watershed has the conditions for DF formation. The first determines whether each small watershed in prediction region is a DF watershed through field observation. The second method is an assessment based on the formation conditions of DFs. Obviously, the first method is the best, but it is too difficult to be carried out for a large region. As we know, there are three necessary conditions for DF formation, including topography, loose solid material and water. Among these, the latter two conditions change rapidly, whereas the topography can be considered as invariable in the long term, and it is the basic condition for the formation of DFs. Therefore, according to the topography of the prediction region, the small watersheds that have the basic conditions for DF formation can be extracted and can be taken as the prediction objects in this system.

Xiong (2013) selected the relative height and area of small watersheds as the identification indexes to determine the watersheds with the possibility of DF occurrences and established an identification model of potential DF watersheds based on energy conditions.

## Application and analysis of debris-flow early warning system in Wenchuan

D. L. Liu et al.

[Title Page](#)

[Abstract](#)

[Introduction](#)

[Conclusions](#)

[References](#)

[Tables](#)

[Figures](#)

[⏪](#)

[⏩](#)

[◀](#)

[▶](#)

[Back](#)

[Close](#)

[Full Screen / Esc](#)

[Printer-friendly Version](#)

[Interactive Discussion](#)



$$\ln(H) - 0.2515 \times \ln(A) - 3.485 > 0 \quad A \in (0.1, 300 \text{ km}^2) \quad (3)$$

where  $H$  (m) is the relative height of a watershed and  $A$  ( $\text{km}^2$ ) is the watershed area. If the relative height and area of a small watershed satisfy Eq. (3), the small watershed has the appropriate conditions for DF formation and can be identified as a potential DF watershed.

Based on the energy conditions, an identification subsystem of the potential DF watersheds was established using GIS and database techniques, which were embedded in this prediction system as an independent module. The identification steps of this subsystem are as follows: (1) the hydrologic modeling is used to extract the small watershed data in raster format from the DEM of the prediction region. (2) The raster-to-polygon tool is used to convert the watershed data into vector format data. (3) The calculate-geometry tool is used to compute the area of each watershed. (4) The extract-by-mask tool is used to obtain the DEM of each watershed, as well as the relative height (the difference between the maximum and minimum elevation values) and area of each watershed. (5) The identification model is used to judge whether each watershed is a potential DF watershed.

3. Simulation of hydrological process in watersheds experiencing rainfall. According to Eq. (2), to use the mixture density  $\rho$  to estimate the formation probability of DFs, the total volume of the unstable soil mass  $v_s$  and runoff  $v_w$  in each potential DF watershed should be calculated in real time. The two volume values are closely linked with the hydrological parameters of the slopes under the action of rainfall, such as the soil water content, matrix suction, infiltration and runoff, which can be obtained by the hydrological process simulation of the watersheds. In this research, the distributed hydrological model GBHM (Yang et al., 1998, 2002; Cong et al., 2009) is employed to simulate the hydrological processes (e.g. interception, infiltration and runoff) in the watersheds experiencing rainfall.

## Application and analysis of debris-flow early warning system in Wenchuan

D. L. Liu et al.

[Title Page](#)

[Abstract](#)

[Introduction](#)

[Conclusions](#)

[References](#)

[Tables](#)

[Figures](#)

[⏪](#)

[⏩](#)

[◀](#)

[▶](#)

[Back](#)

[Close](#)

[Full Screen / Esc](#)

[Printer-friendly Version](#)

[Interactive Discussion](#)



In a certain watershed, the parameters of the slopes, such as the soil cohesive force, internal friction angle and slope gradient, are provided. According to the limit equilibrium Eq. (1), the safety factor ( $F_s$ ) is directly related to the matrix suction of the soil, and the matrix suction is determined by the soil water content. To obtain more accurate hydrological parameters, the initial value of the soil water content in the watersheds should be ensured first. However, under the influence of rainfall infiltration and evapotranspiration, the initial value of soil water content at any time cannot be directly calculated. During the winter in China, the soil water content of topsoil is close to the residual water content. Therefore, in this study, the accurate initial value of the soil water content can be calculated by the hydrological process simulation combined with the meteorological data from 1 January of the prediction year to the prediction time. According to the initial value of the prediction time, the hydrological parameters (e.g. the soil water content and matrix suction) can be assessed by the hydrological process simulation using the radar-predicted precipitation as input.

4. Calculation of the soil–water mixture density in watersheds experiencing rainfall. Taking the soil water content and matrix suction as dynamic inputs, the safety factor ( $F_s$ ) of each soil layer in each grid cell can be calculated by using the limit equilibrium Eq. (1). If  $F_s < 1$ , the soil mass of the soil layer in the grid cell is considered to be unstable. According to the unstable depth in grid cells  $D_{ins}$  estimated by  $F_s$ , the total volume of the unstable soil mass  $v_s$  in each watershed at the time  $t_0$  can be calculated in real time with Eq. (4). Based on the mechanism of runoff generation vs. infiltration, the runoff depth  $D_r$  of grid cells can be estimated by using the Manning formula. According to the  $D_r$  of each grid, the total volume of runoff  $v_w$  in each watershed at the time  $t_0$  can be calculated with Eq. (5). Finally, the density value  $\rho$  of the soil–water mixture in each watershed can be calculated by the water–soil coupling Eq. (2).

## Application and analysis of debris-flow early warning system in Wenchuan

D. L. Liu et al.

[Title Page](#)

[Abstract](#)

[Introduction](#)

[Conclusions](#)

[References](#)

[Tables](#)

[Figures](#)

[⏪](#)

[⏩](#)

[◀](#)

[▶](#)

[Back](#)

[Close](#)

[Full Screen / Esc](#)

[Printer-friendly Version](#)

[Interactive Discussion](#)



$$v_s = \sum_{t=1}^{t=t_0} \sum_{i=1}^{N_{\text{ins}}} S_i \times D_{\text{ins}} \quad (4)$$

where  $v_s$  ( $\text{m}^3$ ) is the total volume of the unstable soil mass at the time  $t_0$ ,  $D_{\text{ins}}$  (m) is the unstable depth of each grid,  $S_i$  ( $\text{m}^2$ ) is the area of each grid, and  $N_{\text{ins}}$  is the total quantity of the unstable grids at the time  $t_0$ .

$$v_w = \sum_{t=1}^{t=t_0} \sum_{i=1}^N S_i \times D_r \quad (5)$$

where  $v_w$  ( $\text{m}^3$ ) is the total volume of runoff at the time  $t_0$ ,  $D_r$  (m) is the runoff depth of each grid,  $S_i$  ( $\text{m}^2$ ) is the area of each grid, and  $N$  is the total number of grids in each watershed.

5. Estimation of the probability of DF formation in the watersheds. By comparing the density value  $\rho$  of the soil–water mixture within each potential DF watershed with Table 1, the probability interval and the warning level of DF formation within each potential DF watershed can be determined. According to the different warning levels, each potential DF watershed can be marked with a corresponding color, and the early warning information can be published.

## 4 DF predictions within the Wenchuan earthquake-affected area

### 4.1 Preparation of basic data

1. Data for the hydrological process simulation. The hydrological process simulation is performed by using grid cells as the basic units. More grid cells mean lower

## Application and analysis of debris-flow early warning system in Wenchuan

D. L. Liu et al.

[Title Page](#)

[Abstract](#)

[Introduction](#)

[Conclusions](#)

[References](#)

[Tables](#)

[Figures](#)

[⏪](#)

[⏩](#)

[◀](#)

[▶](#)

[Back](#)

[Close](#)

[Full Screen / Esc](#)

[Printer-friendly Version](#)

[Interactive Discussion](#)



computational efficiency but higher prediction precision and vice versa. To improve the prediction efficiency and ensure that the prediction precision meets the demand, a compromise should be found for this problem. Because the commonly used DEM resolutions are 30, 90 and 250 m and the area of each DF watershed is 0.1–300 km<sup>2</sup>, the data of the potential DF watersheds are converted into data with a resolution of 250 m × 250 m by the resample tool in ArcGIS. By overlaying the potential DF watershed data and the regional DEM (250 m × 250 m), the elevation information of each potential DF watershed can be obtained.

The original underlying surface data, such as land use type, soil type and soil depth, in this region can be obtained from the FAO database (<http://www.fao.org/geonetwork/srv/en/main.home>). These data are also converted into raster data (Fig. 5) with the same resolution as the DEM via the resample tool and Extract by Mask feature in ArcGIS. The main land use types in this region are forest land, farm land, shrub land and slope cropland, as shown in Table 2. There are 11 soil types and 2 soil depth types (1 and 4 m) in this region. The characteristic soil hydraulic parameters of each soil type and the soil depth information are shown in Tables 3 and 4, respectively.

- Soil mechanics parameters in the earthquake-affected area. The approach to assess the soil mechanical parameters in the earthquake-affected area consists of three steps. Based on the geological map of earthquake-affected area, the lithology of the region can be obtained. Based on the handbook of rock mechanics, the mechanical parameters (such as the soil cohesion  $c$  and the internal friction angle  $\varphi$ ) values of the corresponding lithology can be assigned. These mechanical parameter values are also converted into the raster data (Fig. 6) with a resolution corresponding to the DEM.

## 4.2 Identification of potential DF watersheds

With the DEM of the earthquake-affected area as the input, the identification subsystem of potential DF watersheds can extract the potential DF watersheds in this region. The identification results show that there are 631 potential DF watersheds in this region.

5 As shown in Fig. 7, we compared the identification result (polygon data) and the 669 identified DF watersheds (point data) based on the field observation. In total, 98.7 % of the identified DF watersheds are located in the potential DF watersheds, and certain identified DF watersheds may be located in the same potential DF watershed. Some missing points are near the edge of the potential DF watersheds, and the other missing  
10 points are almost located in the Sichuan Basin.

## 4.3 Input of dynamic data

1. Input of meteorological data. The original meteorological data, including from the 65 weather stations in the earthquake-affected area and nearby regions (Fig. 8), are provided by the Weather Bureau of Sichuan Province. The meteorological data from each weather station are composed of measured rainfall, temperature (maximum, mean and minimum temperature), wind velocity, relative humidity and sunshine time. According to the coordinate information of each weather station, these data are converted into raster data with a resolution corresponding to the DEM via the Kriging spatial interpolation method.
- 15 2. Input of radar-predicted precipitation data. The original predicted precipitation data in the earthquake-affected area on 17 August 2012 are provided by the Weather Bureau of Sichuan Province, but they do not meet the demand of this prediction system directly. The predicted precipitation data for this prediction system should have the same resolution and coverage area as the DEM of this region. Therefore, according to the original predicted precipitation data and this regional  
20 DEM, the predicted precipitation data for this prediction system can be generated

by the tools of Add XY Data, Feature to Raster, Resample and Extract by Mask in ArcGIS (Fig. 9).

#### 4.4 Results and analysis of the prediction

The formation probability and the warning level of each potential DF watershed in the earthquake-affected area were predicted for 17 August 2012 by the DF prediction system based on the water–soil coupling mechanism. The prediction results at 19:00 (Beijing time zone) are shown in Fig. 10. According to the DF events reported by the Land and Resources Department of Sichuan Province, 156 watersheds experienced DFs in the Wenchuan earthquake-affected area. The results of this prediction system show that there are 161 watersheds that are at risk of DFs. In the comparison of the prediction results and the actual DF events, DF events in 127 watersheds were predicted successfully and 29 watersheds were not predicted to have DFs. Additionally, 34 watersheds were predicted by the system to have DFs that in fact did not experience DFs. Thus, the rate of prediction failures (in which DFs occurred but were not predicted) is 19 %, and the rate of false predictions (in which DFs are predicted, but no DFs occurred) is 21 %. Further analysis of the watersheds with prediction failures shows that there are 4 watersheds (labeled as “Unsuccessful watersheds: 1” in Fig. 10) that are not classified as potential DF watersheds, and that the 24 h of cumulative precipitation is less than 20 mm in 6 watersheds (labeled as “Unsuccessful watersheds: 2” in Fig. 10). If the 10 watersheds with prediction failures are excluded for the two reasons, it will be 19 watersheds with prediction failures (labeled as “Unsuccessful watersheds: 3” in Fig. 10). It is here concluded the real rate of prediction failures for the system is only 12 %. As for the 34 watersheds with false predictions, parts of them were actually caused by the precision of Radar prediction rainfall. The Radar prediction precipitation in the 16 watersheds with false predictions was almost larger than 100 mm on the prediction day. As a consequence, the warning level generated by the system ranged from green color to orange color with the Radar prediction rainfall as input. But the observed rainfall (Fig. 11) in these 16 watersheds was less than 10 mm (labeled as “Watersheds:

### Application and analysis of debris-flow early warning system in Wenchuan

D. L. Liu et al.

[Title Page](#)

[Abstract](#)

[Introduction](#)

[Conclusions](#)

[References](#)

[Tables](#)

[Figures](#)

[⏪](#)

[⏩](#)

[◀](#)

[▶](#)

[Back](#)

[Close](#)

[Full Screen / Esc](#)

[Printer-friendly Version](#)

[Interactive Discussion](#)



false-prediction” in Fig. 11), which was far smaller than the Radar prediction precipitation and difficult to trigger DFs in these watersheds in fact. So, if the 16 watersheds with false predictions are excluded for this reason, it will be 18 watersheds with false predictions, and the real rate of false predictions for the system is only 11 %.

5 The formation probability of DFs in this region on that day is also forecast by the prediction system based on the DF contribution factors in the Weather Bureau of Sichuan Province. This system divides the critical rainfall into a series of grade intervals according to the different conditions of DF formation and utilizes the method of fuzzy mathematics to determine the formation probability of DFs based on the predicted precipitation interval range and the underlying surface conditions (Wei et al., 2006, 2007).  
10 The prediction results on 17 August 2012 are shown in Fig. 12.

According to the Fig. 12, the expression mode of the warning level in the prediction system based on the DF contribution factors is entirely grid-unit based. But DF generally occurred in a relatively small watershed (Wei et al., 2008), and the grid unit is difficult to express the morphology of a DF watershed. So the expression format using the grid unit should be replaced by the watershed unit. There are two rules to govern the above transforming process including the rule of highest warning level (the warning level of a watershed corresponds to the grids that have the highest warning level within the watershed) and the rule of most warning level (the warning level of a watershed corresponds to grids with the same and dominated warning level within the watershed).  
15 Figures 13 and 14 indicate that some watersheds could even have two different warning levels by following the above two rules, so the transforming results are quite uncertain. Additionally, this transforming process need lots of manual works, and it is hence not beneficial to the operation prediction for DFs.

25 The prediction results obtained by the above two prediction systems are compared here to test the capacity of our proposed system. The comparison results listed in Table 5 indicate that the prediction results of our system are quite excellent, whose failure prediction rate and false prediction rate are 19 and 21 % lower than the system based on the DF contribution factors (32 and 45 %), respectively.

**Application and analysis of debris-flow early warning system in Wenchuan**

D. L. Liu et al.

[Title Page](#)

[Abstract](#)

[Introduction](#)

[Conclusions](#)

[References](#)

[Tables](#)

[Figures](#)

[⏪](#)

[⏩](#)

[⏴](#)

[⏵](#)

[Back](#)

[Close](#)

[Full Screen / Esc](#)

[Printer-friendly Version](#)

[Interactive Discussion](#)



Discussion Paper | Discussion Paper | Discussion Paper | Discussion Paper | Discussion Paper

## 5 Applications of new prediction system in Sichuan weather Bureau

Due to advantages of the new prediction system comparing to the one that currently used in operational forecasting works, the new system was installed in Sichuan Weather Bureau before the rainy season the Wenchuan earth quake-affected area in 2013. Two prediction results of 9 July 2013 and 10 July 2014 generated by the new prediction system are respectively shown in Fig. 15. The failure prediction rate and false prediction rate of the prediction result for 9 July 2013 is 16 and 22 %, respectively (Table 6).

The DF events in 2014 were not very remarkable, and the exact information of DF events (e.g. the time and place) is not available for this research. However, there is still some helpful information of DF events that can be collected from Internet. For example, on 10 July of 2014, it was reported that there were DF events in six townships in Lixian County, one town in Xiaojin County and three towns in Wenchuan County. The radar rainfall on 10 July 2014 was used in the new prediction system. The prediction results of DF shown in Fig. 15b show a good agreement with the reported information on Internet ([http://www.qimaren.com/news/2014/07/10\\_3104.html](http://www.qimaren.com/news/2014/07/10_3104.html)). The operational forecasting works in the years of 2013 and 2014 demonstrated that the new prediction system installed in the Weather Bureau of Sichuan province had an excellent operational stability with a high prediction capacity and precision.

## 6 Discussion and conclusions

A new physics-based EWS for DF forecasting has been developed and installed in the Weather Bureau of Sichuan province. The three typical cases studies demonstrated that this new EWS has a high operational stability with high prediction accuracy. However, there are three problems in the new EWS that need to be studied further. The first, the hydrological simulation with large amount calculations in this system is so complicated that it will be a time-consuming prediction process. The calculation of the initial

## Application and analysis of debris-flow early warning system in Wenchuan

D. L. Liu et al.

[Title Page](#)

[Abstract](#)

[Introduction](#)

[Conclusions](#)

[References](#)

[Tables](#)

[Figures](#)

[⏪](#)

[⏩](#)

[◀](#)

[▶](#)

[Back](#)

[Close](#)

[Full Screen / Esc](#)

[Printer-friendly Version](#)

[Interactive Discussion](#)



## Application and analysis of debris-flow early warning system in Wenchuan

D. L. Liu et al.

[Title Page](#)

[Abstract](#)

[Introduction](#)

[Conclusions](#)

[References](#)

[Tables](#)

[Figures](#)

[⏪](#)

[⏩](#)

[◀](#)

[▶](#)

[Back](#)

[Close](#)

[Full Screen / Esc](#)

[Printer-friendly Version](#)

[Interactive Discussion](#)

soil water content value for DF prediction is especially time intensive and thus hard to meet the demand of an operational prediction because this calculation process is from 1 January to the prediction time with a calculation step of 1 h. To improve the prediction efficiency, the above initial value calculation process can be replaced by the method of effective antecedent rainfall. If so, the identification of the initial value of the soil water content will only require the rainfall data for the 15 days prior to the prediction time; the second, in this system, the total volume of unstable soil mass is used to calculate the density of the water–soil mixture within a watershed. It is assumed that once the soil mass failed, all of it will move into the watershed channel and participate in the water–soil coupling process. However, portions of the unstable soil mass may stay on slopes instead of moving into the channel, and this will cause density values calculated by this system to be larger than the real case. To obtain more accurate density values, the movement process of the unstable soil mass needs to be studied further; the third, the density of the water–soil mixture is used to quantitatively characterize the complex dynamic formation process of DFs in this system. Therefore, this method cannot completely describe this complex dynamic process and belongs to a grey-box model. To reflect the formation of DFs at the watershed scale more completely, the dynamic DF formation process in watersheds needs to be studied further; and the last, there are two supplement patterns of material source for DF formation, rainfall-induced landslides from slopes in watersheds and deposits in channel bed eroded by the runoff. The theory of this prediction system is based on the coupling of runoff and solid material from rainfall-induced landslides. Obviously, this prediction system will not work well for predicting DFs with the other supplement pattern of material source.

*Acknowledgement.* This research was supported by the foundation of the Research Fund for Commonweal Trades (Meteorology) (No.GYHY201006039), National Science and Technology Support Program (2011BAK12B00), International Cooperation Project of the Department of Science and Technology of Sichuan Province (No. 2009HH0005) and National Natural Science Foundation of China (No. 41501114). We appreciate the Weather Bureau of Sichuan Province for the data services.

## References

- Aletti, P.: A warning system for rainfall-induced shallow failures, *Eng. Geol.*, 73, 247–265, 2004.
- Badoux, A., Turowski, J. M., Mao, L., Mathys, N., and Rickenmann, D.: Rainfall intensity–duration thresholds for bedload transport initiation in small Alpine watersheds, *Nat. Hazards Earth Syst. Sci.*, 12, 3091–3108, doi:10.5194/nhess-12-3091-2012, 2012.
- 5 Berenguer, M., Sempere-Torres, D., and Hürlimann, M.: Debris-flow forecasting at regional scale by combining susceptibility mapping and radar rainfall, *Nat. Hazards Earth Syst. Sci.*, 15, 587–602, doi:10.5194/nhess-15-587-2015, 2015.
- Borga, M., Stoffel, M., Marchi, L., Marra, F., and Jakob, M.: Hydrogeomorphic response to extreme rainfall in headwater systems: flash floods and debris flows, *J. Hydrol.*, 518, 194–205, 2014.
- 10 Caine, N. The rainfall intensity-duration control of shallow landslides and debris flows, *Geogr. Ann. A*, 62, 23–27, 1980.
- Chen, H. and Lee, C. F.: Geohazards of slope mass movement and its prevention in Hong Kong, *Eng. Geol.*, 76, 3–25, 2004.
- 15 Cui, P.: Experiment research of the initial condition and mechanism of debris flow, *Chinese Sci. Bull.*, 21, 1650–1652, 1991.
- European Commission D. G. Environment: Member States’ approaches towards prevention policy - a critical analysis, Final Report, 2008.
- 20 Gariano, S. L., Brunetti, M. T., Iovine, G., Melillo, M., Peruccacci, S., Terranova, O., Vennari, C., and Guzzetti, F.: Calibration and validation of rainfall thresholds for shallow landslides forecasting in Sicily, Southern Italy, *Geomorphology*, 228, 653–665, doi:10.1016/j.geomorph.2014.10.019, 2015.
- Giannecchini, R., Galanti, Y., and D’Amato Avanzi, G.: Critical rainfall thresholds for triggering shallow landslides in the Serchio River Valley (Tuscany, Italy), *Nat. Hazards Earth Syst. Sci.*, 25 12, 829–842, doi:10.5194/nhess-12-829-2012, 2012.
- Guzzetti, F., Peruccacci, S., Rossi, M., and Stark, C. P.: Rainfall thresholds for the initiation of landslides in central and southern Europe, *Meteorol. Atmos. Phys.*, 98, 239–267, 2007.
- Guzzetti, F., Peruccacci, S., Rossi, M., and Stark, C. P.: The rainfall intensity-duration control of shallow landslides and debris flow: an update, *Landslides*, 5, 3–17, 2008.
- 30 Iverson, R. M., Reid, M. E., and LaHusen, R. G.: Debris-flow mobilization from landslides, *Ann. Rev. Earth Planet. Sci.*, 25, 85–138, 1997.

## Application and analysis of debris-flow early warning system in Wenchuan

D. L. Liu et al.

[Title Page](#)

[Abstract](#)

[Introduction](#)

[Conclusions](#)

[References](#)

[Tables](#)

[Figures](#)

[I◀](#)

[▶I](#)

[◀](#)

[▶](#)

[Back](#)

[Close](#)

[Full Screen / Esc](#)

[Printer-friendly Version](#)

[Interactive Discussion](#)



## Application and analysis of debris-flow early warning system in Wenchuan

D. L. Liu et al.

[Title Page](#)

[Abstract](#)

[Introduction](#)

[Conclusions](#)

[References](#)

[Tables](#)

[Figures](#)

[⏪](#)

[⏩](#)

[◀](#)

[▶](#)

[Back](#)

[Close](#)

[Full Screen / Esc](#)

[Printer-friendly Version](#)

[Interactive Discussion](#)

- Kang, Z. C.: The mechanical analysis of the generation of debris flow, *Mt. Res.*, 5, 225–230, 1987.
- Kang, Z. C., Li, C. F., and Ma, A. N.: Debris flow Research in China, Science Press, Beijing, 21–22, 2004.
- 5 Osanai, N., Shimuzu, T., Kuramoto, K., and Noro, T.: Japanese early-warning for debris flows and slopes failures using rainfall indices with radial basis function network, *Landslides*, 7, 325–338, 2010.
- Papa, M. N., Medina, V., Ciervo, F., and Bateman, A.: Derivation of critical rainfall thresholds for shallow landslides as a tool for debris flow early warning systems, *Nat. Hazards Earth Syst. Sci.*, 17, 4095–4107, 2013,  
 10 <http://www.nat-hazards-earth-syst-sci.net/17/4095/2013/>.
- Tang, C., Zhu, J., Li, W. L., and Liang, J. T.: Rainfall-triggered debris flows following the Wenchuan earthquake, *B. Eng. Geol. Environ.*, 68, 187–194, 2009.
- Vennari, C., Gariano, S. L., Antronico, L., Brunetti, M. T., Iovine, G., Peruccacci, S., Terranova, O., and Guzzetti, F.: Rainfall thresholds for shallow landslide occurrence in Calabria, southern Italy, *Nat. Hazards Earth Syst. Sci.*, 14, 317–330, doi:10.5194/nhess-14-317-2014,  
 15 2014.
- Wei, F. Q., Tang, J. F., Xie, H., and Zhong, D. L.: Debris flow forecast combined regions and valleys and its application, *J. Mt. Sci.*, 22, 321–325, 2004.
- 20 Wei, F. Q., Gao, K. C., Cui, P., Hu, K., Xu, J., Zhang, G., and Bi, B.: Method of debris flow prediction based on a numerical weather forecast and its application, in: *Monitoring, Simulation, Prevention and Remediation of Dense and Debris Flow*, edited by: G. Lorenzini, Brebbia, C. A., Emmanouloudis, D. E., WIT Press, Southampton, 37–46, 2006.
- Wei, F. Q., Gao, K. C., Jiang, Y. H., Jia, S. W., Cui, P., Xu, J., Zhang, G. P., and Bi, B. G.: GIS-based prediction of debris flows and landslides in southwestern China, in: *Proceedings of Debris-Flow Hazards Mitigation: Mechanics, Prediction, and Assessment*, edited by: Chen, C. L. and Major, J. J., Mill Press, Netherlands, 479–490, 2007.
- 25 Wei, F. Q., Su, P. C., and Jiang, Y. H.: Distribution characteristics of landslides and debris flows in the wenchuan earthquake region before and after the Earthquake, *Disaster Advances*, 5, 285–294, 2012.
- 30 Xie, H., Zhong, D. L., Jiao, Z., and Zhang, J. S.: Debris flow in Wenchuan quake-hit area in 2008, *J. Mt. Sci.*, 27, 501–509, 2009.

- Zhang, S. J., Yang, H. J., Wei, F. Q., Jiang, Y. H., and Liu, D. L.: A model of debris flow forecast based on the water–soil coupling mechanism, *J. Earth Sci.*, 25, 757–763, 2014a.
- Zhang, S. J., Wei, F. Q., Liu, D. L., Yang, H. J., and Jiang, Y. H.: A regional-scale method of forecasting debris flow events based on water–soil coupling mechanism, *J. Mt. Sci.*, 11, 1531–1542, 2014b.
- Zhang, S. J., Wei, F. Q., Liu, D. L., and Jiang, Y. H.: Analysis of slope stability based on the limit equilibrium equation and the hydrological simulation, *J. Basic Sci. Eng.*, in press, 2015.
- Zhong, D. L., Xie, H., and Wei, F. Q.: *Map of Debris Flow Distribution and Danger Degree Division in Sichuan and Chongqing and Its Manual*, Chengdu Cartographic Publishing House, Chengdu, 1997.

## Application and analysis of debris-flow early warning system in Wenchuan

D. L. Liu et al.

Title Page

Abstract

Introduction

Conclusions

References

Tables

Figures

⏪

⏩

◀

▶

Back

Close

Full Screen / Esc

Printer-friendly Version

Interactive Discussion



## Application and analysis of debris-flow early warning system in Wenchuan

D. L. Liu et al.

**Table 1.** Formation probability of DFs according to the water–soil mixture density.

Standard DF density (gcm <sup>3</sup> )	$\rho < 1.2$	$\rho = 1.2\text{--}1.5$	$\rho = 1.5\text{--}1.8$	$\rho = 1.8\text{--}2.0$	$\rho = 2.0\text{--}2.3$
Formation probability of DFs (%)	0–20	20–40	40–60	60–80	80–100
Level of early warning	1	2	3	4	5
Color of early warning	Green	Blue	Yellow	Orange	Red

[Title Page](#)

[Abstract](#)

[Introduction](#)

[Conclusions](#)

[References](#)

[Tables](#)

[Figures](#)

[I◀](#)

[▶I](#)

[◀](#)

[▶](#)

[Back](#)

[Close](#)

[Full Screen / Esc](#)

[Printer-friendly Version](#)

[Interactive Discussion](#)

## Application and analysis of debris-flow early warning system in Wenchuan

D. L. Liu et al.

[Title Page](#)

[Abstract](#)

[Introduction](#)

[Conclusions](#)

[References](#)

[Tables](#)

[Figures](#)

[|◀](#)

[▶|](#)

[◀](#)

[▶](#)

[Back](#)

[Close](#)

[Full Screen / Esc](#)

[Printer-friendly Version](#)

[Interactive Discussion](#)

**Table 2.** The land use type information in the earthquake-affected area.

Number of land use type	Name of land use type	Percentage of area/%
1	water body	0.43 %
2	urban area	0.69 %
3	bare land	0.16 %
4	forest land	27.37 %
5	upland	7.36 %
6	slope cropland	15.95 %
7	farm land	26.34 %
8	shrub land	21.51 %
9	wet land	0.14 %
10	snow land	0.05 %



## Application and analysis of debris-flow early warning system in Wenchuan

D. L. Liu et al.

[Title Page](#)

[Abstract](#)

[Introduction](#)

[Conclusions](#)

[References](#)

[Tables](#)

[Figures](#)

[|◀](#)

[▶|](#)

[◀](#)

[▶](#)

[Back](#)

[Close](#)

[Full Screen / Esc](#)

[Printer-friendly Version](#)

[Interactive Discussion](#)

**Table 4.** The soil depth information in earthquake-affected area.

Depth/m	Percentage of area/%	Depth of each soil layer/m						
		1	2	3	4	5	6	7
1	43.5 %	0.025	0.05	0.75	0.1	0.15	0.25	0.35
4	56.5 %	0.1	0.2	0.3	0.4	0.6	1.0	1.4

## Application and analysis of debris-flow early warning system in Wenchuan

D. L. Liu et al.

**Table 5.** Comparison of the prediction results of the two systems.

prediction system	water–soil coupling mechanism	contribution factors
Number of watersheds with predicted DFs	161	192
Number of watersheds with actual DFs	156	156
Number of watersheds with both predicted and actual DFs	127	106
Number of watersheds with DF prediction failures	29	50
Number of false prediction watersheds	34	86
Prediction failure rate	19%	32%
False prediction rate	21%	45%

[Title Page](#)

[Abstract](#)

[Introduction](#)

[Conclusions](#)

[References](#)

[Tables](#)

[Figures](#)

[|◀](#)

[▶|](#)

[◀](#)

[▶](#)

[Back](#)

[Close](#)

[Full Screen / Esc](#)

[Printer-friendly Version](#)

[Interactive Discussion](#)

## Application and analysis of debris-flow early warning system in Wenchuan

D. L. Liu et al.

[Title Page](#)

[Abstract](#)

[Introduction](#)

[Conclusions](#)

[References](#)

[Tables](#)

[Figures](#)

[|◀](#)

[▶|](#)

[◀](#)

[▶](#)

[Back](#)

[Close](#)

[Full Screen / Esc](#)

[Printer-friendly Version](#)

[Interactive Discussion](#)



**Table 6.** Analysis table of the forecast results on 9 July 2013.

Number of watersheds with predicted DFs	169
Number of watersheds with actual DFs	157
Number of watersheds with both predicted and actual DFs	132
Number of watersheds with DF prediction failures	25
Number of false prediction watersheds	37
Prediction failure rate	16%
False prediction rate	22%

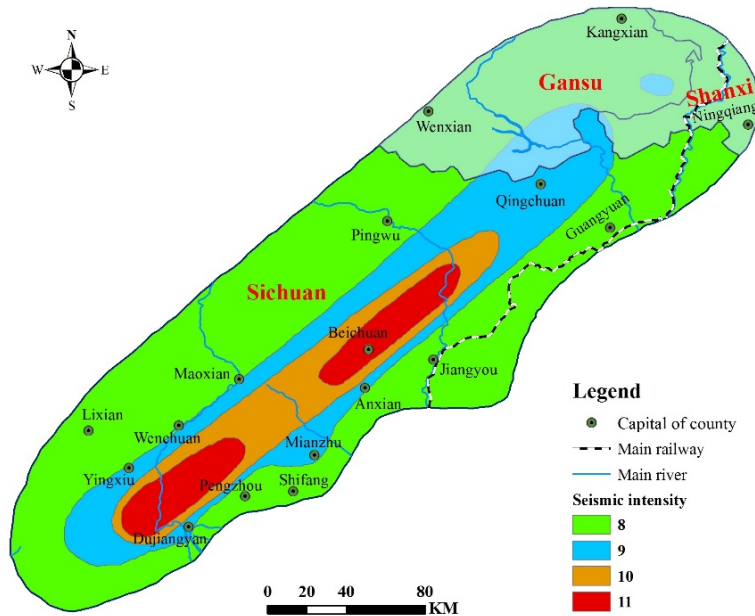


Figure 1. Map of 2008 Wenchuan earthquake-affected area.

**Application and analysis of debris-flow early warning system in Wenchuan**

D. L. Liu et al.

[Title Page](#)

[Abstract](#)

[Introduction](#)

[Conclusions](#)

[References](#)

[Tables](#)

[Figures](#)

⏪

⏩

◀

▶

[Back](#)

[Close](#)

[Full Screen / Esc](#)

[Printer-friendly Version](#)

[Interactive Discussion](#)



## Application and analysis of debris-flow early warning system in Wenchuan

D. L. Liu et al.

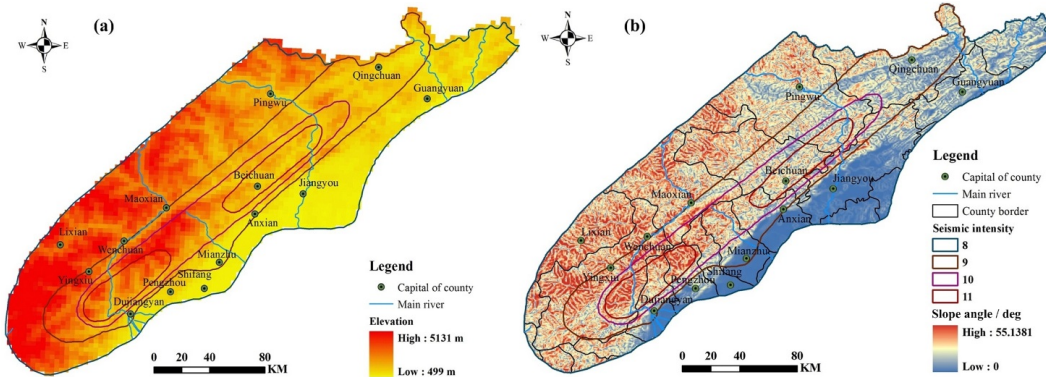


**Figure 2.** (a) Elevation of the earthquake-affected area; (b) slope angle of the earthquake-affected area.

<a href="#">Title Page</a>	
<a href="#">Abstract</a>	<a href="#">Introduction</a>
<a href="#">Conclusions</a>	<a href="#">References</a>
<a href="#">Tables</a>	<a href="#">Figures</a>
<a href="#">⏪</a>	<a href="#">⏩</a>
<a href="#">⏴</a>	<a href="#">⏵</a>
<a href="#">Back</a>	<a href="#">Close</a>
<a href="#">Full Screen / Esc</a>	
<a href="#">Printer-friendly Version</a>	
<a href="#">Interactive Discussion</a>	

## Application and analysis of debris-flow early warning system in Wenchuan

D. L. Liu et al.

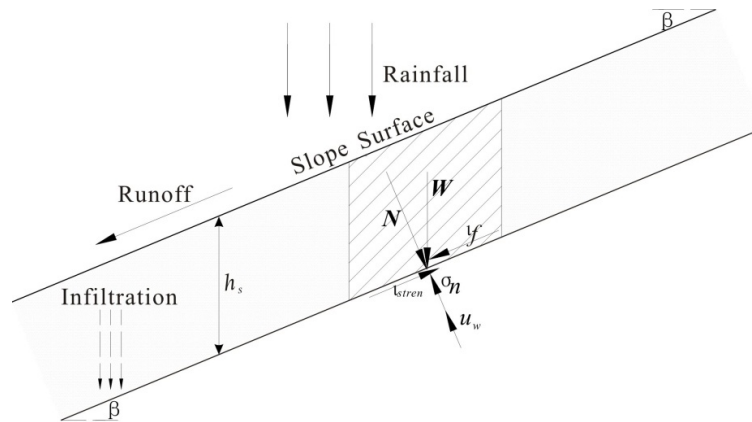


**Figure 3.** Analysis of soil mass stability influenced by rainfall infiltration.

[Title Page](#)

[Abstract](#)

[Introduction](#)

[Conclusions](#)

[References](#)

[Tables](#)

[Figures](#)

[◀](#)

[▶](#)

[◀](#)

[▶](#)

[Back](#)

[Close](#)

[Full Screen / Esc](#)

[Printer-friendly Version](#)

[Interactive Discussion](#)

## Application and analysis of debris-flow early warning system in Wenchuan

D. L. Liu et al.

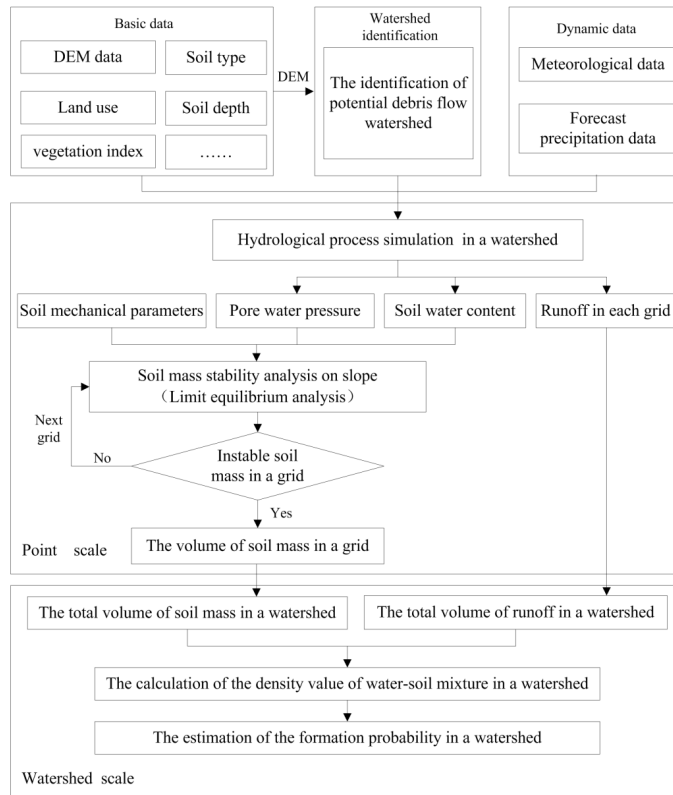


**Figure 4.** Prediction process of the debris-flow prediction system based on water–soil coupling mechanism.

[Title Page](#)  
[Abstract](#)   [Introduction](#)  
[Conclusions](#)   [References](#)  
[Tables](#)   [Figures](#)  
[⏪](#)   [⏩](#)  
[⏴](#)   [⏵](#)  
[Back](#)   [Close](#)  
[Full Screen / Esc](#)  
[Printer-friendly Version](#)  
[Interactive Discussion](#)



## Application and analysis of debris-flow early warning system in Wenchuan

D. L. Liu et al.

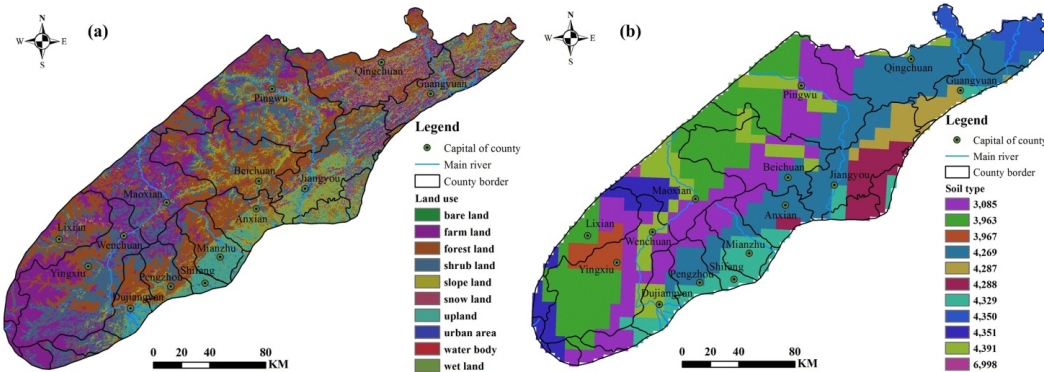


**Figure 5.** (a) Distribution of land use; (b) distribution of soil type.

Title Page	
Abstract	Introduction
Conclusions	References
Tables	Figures
◀	▶
◀	▶
Back	Close
Full Screen / Esc	
Printer-friendly Version	
Interactive Discussion	

## Application and analysis of debris-flow early warning system in Wenchuan

D. L. Liu et al.

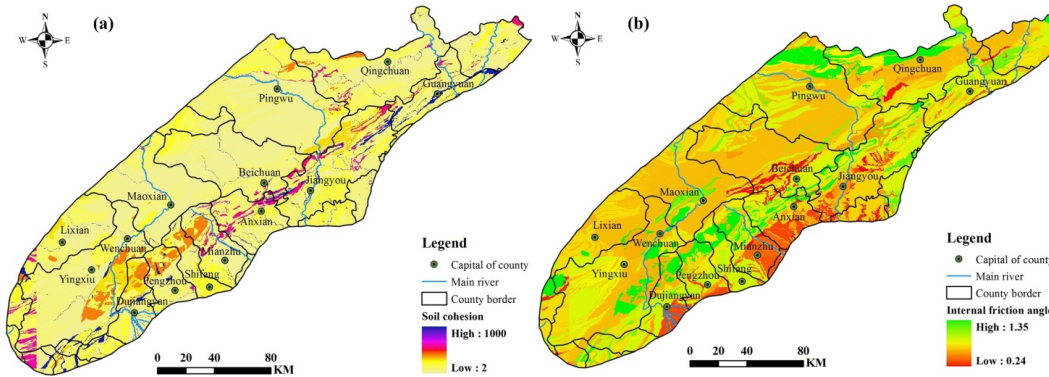


**Figure 6.** (a) Distribution of the soil cohesion values/kPa; (b) distribution of the internal friction angle values.

Title Page	
Abstract	Introduction
Conclusions	References
Tables	Figures
◀	▶
◀	▶
Back	Close
Full Screen / Esc	
Printer-friendly Version	
Interactive Discussion	

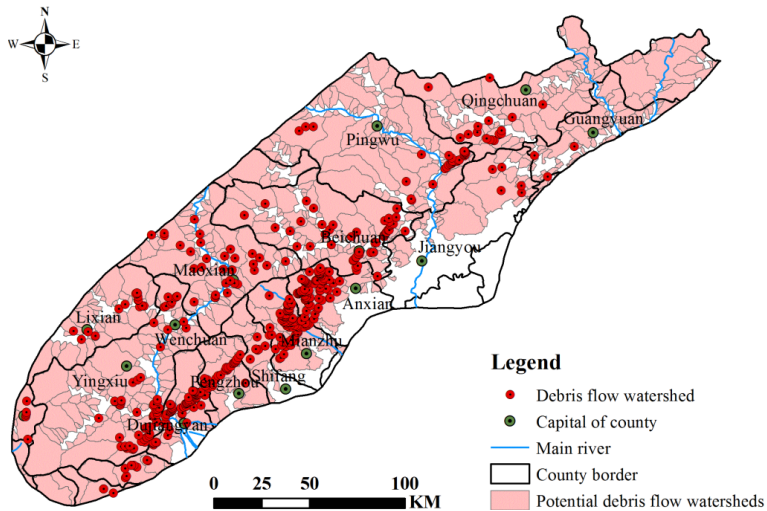


**Figure 7.** Map of the DF watersheds and potential DF watersheds.

**Application and analysis of debris-flow early warning system in Wenchuan**

D. L. Liu et al.

[Title Page](#)

[Abstract](#) [Introduction](#)

[Conclusions](#) [References](#)

[Tables](#) [Figures](#)

[⏪](#) [⏩](#)

[◀](#) [▶](#)

[Back](#) [Close](#)

[Full Screen / Esc](#)

[Printer-friendly Version](#)

[Interactive Discussion](#)



## Application and analysis of debris-flow early warning system in Wenchuan

D. L. Liu et al.

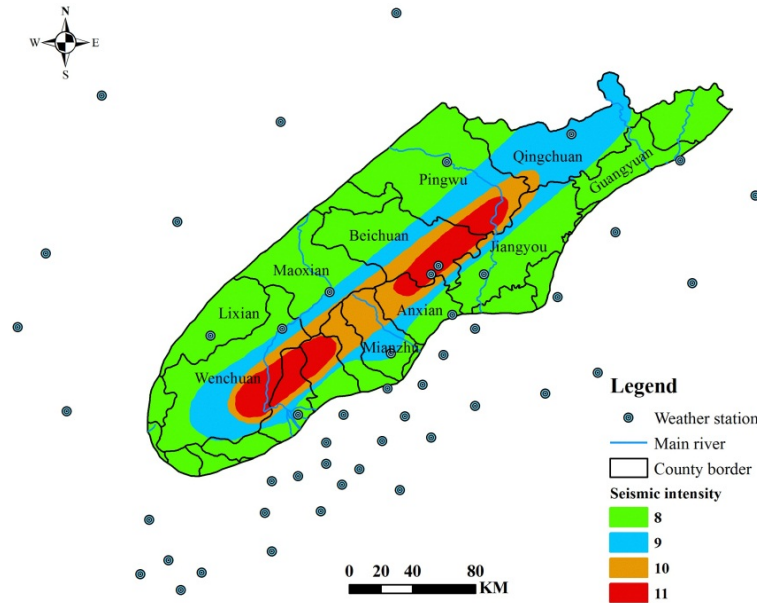


**Figure 8.** Distribution of weather stations in the earthquake-affected area and nearby regions.

[Title Page](#)

[Abstract](#)

[Introduction](#)

[Conclusions](#)

[References](#)

[Tables](#)

[Figures](#)

[⏪](#)

[⏩](#)

[⏴](#)

[⏵](#)

[Back](#)

[Close](#)

[Full Screen / Esc](#)

[Printer-friendly Version](#)

[Interactive Discussion](#)

## Application and analysis of debris-flow early warning system in Wenchuan

D. L. Liu et al.

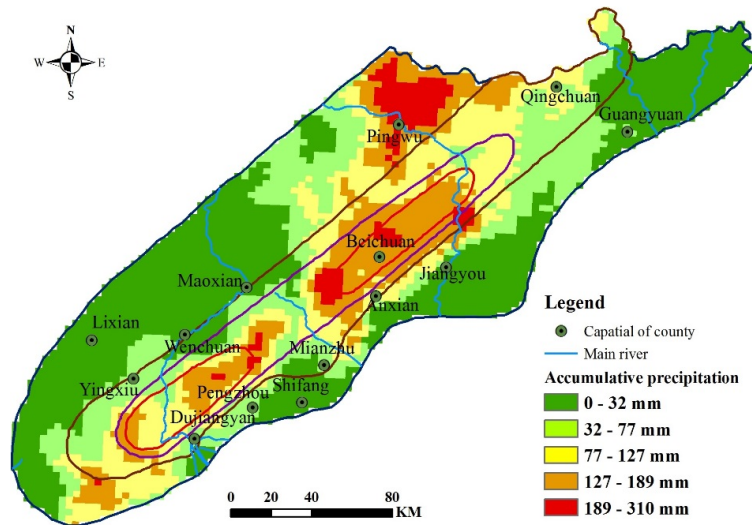


**Figure 9.** Predicted distribution of 24 h of cumulative precipitation.

<a href="#">Title Page</a>	
<a href="#">Abstract</a>	<a href="#">Introduction</a>
<a href="#">Conclusions</a>	<a href="#">References</a>
<a href="#">Tables</a>	<a href="#">Figures</a>
<a href="#">⏪</a>	<a href="#">⏩</a>
<a href="#">⏴</a>	<a href="#">⏵</a>
<a href="#">Back</a>	<a href="#">Close</a>
<a href="#">Full Screen / Esc</a>	
<a href="#">Printer-friendly Version</a>	
<a href="#">Interactive Discussion</a>	



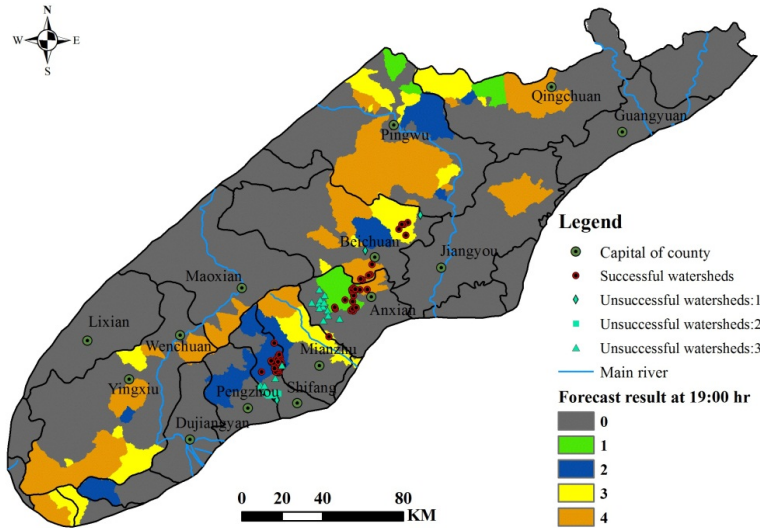


**Figure 10.** Prediction results of the debris-flow prediction system based on the water–soil coupling mechanism.

**Application and analysis of debris-flow early warning system in Wenchuan**

D. L. Liu et al.

[Title Page](#)

[Abstract](#) [Introduction](#)

[Conclusions](#) [References](#)

[Tables](#) [Figures](#)

[⏪](#) [⏩](#)

[◀](#) [▶](#)

[Back](#) [Close](#)

[Full Screen / Esc](#)

[Printer-friendly Version](#)

[Interactive Discussion](#)



## Application and analysis of debris-flow early warning system in Wenchuan

D. L. Liu et al.

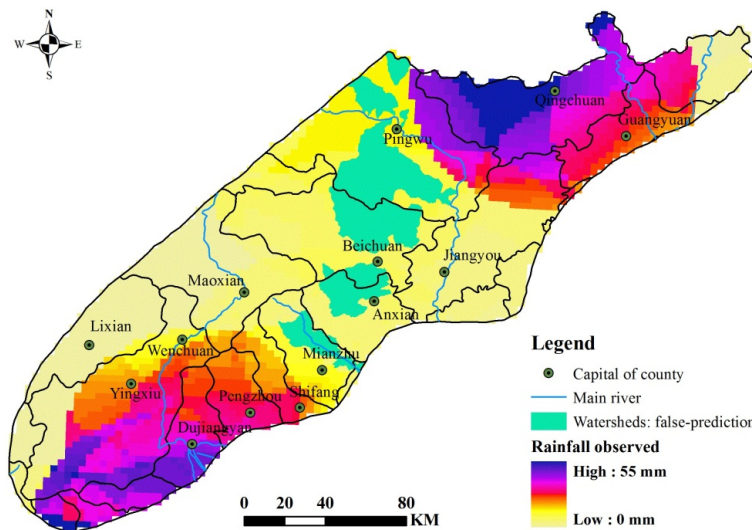


**Figure 11.** Distribution of observed rainfall for the prediction day in the earthquake-affected area.

[Title Page](#)

[Abstract](#)

[Introduction](#)

[Conclusions](#)

[References](#)

[Tables](#)

[Figures](#)

⏪

⏩

◀

▶

[Back](#)

[Close](#)

[Full Screen / Esc](#)

[Printer-friendly Version](#)

[Interactive Discussion](#)



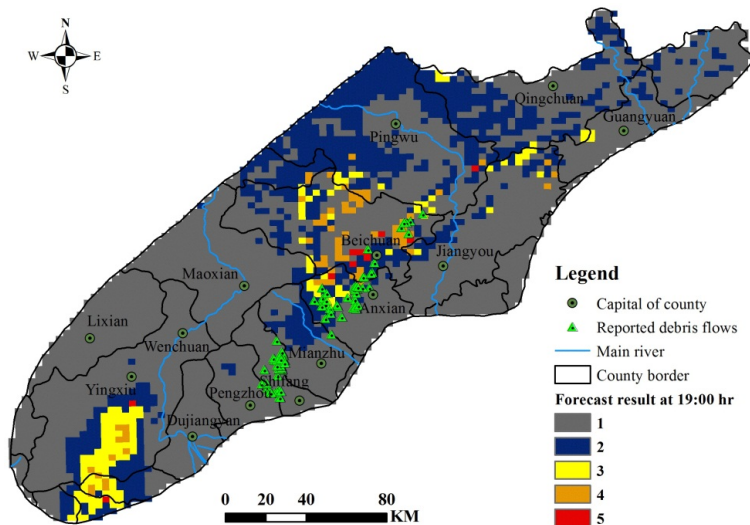


**Figure 12.** Prediction results of the debris-flow prediction system based on contribution factors.

**Application and analysis of debris-flow early warning system in Wenchuan**

D. L. Liu et al.

[Title Page](#)

[Abstract](#)

[Introduction](#)

[Conclusions](#)

[References](#)

[Tables](#)

[Figures](#)

[⏪](#)

[⏩](#)

[⏴](#)

[⏵](#)

[Back](#)

[Close](#)

[Full Screen / Esc](#)

[Printer-friendly Version](#)

[Interactive Discussion](#)



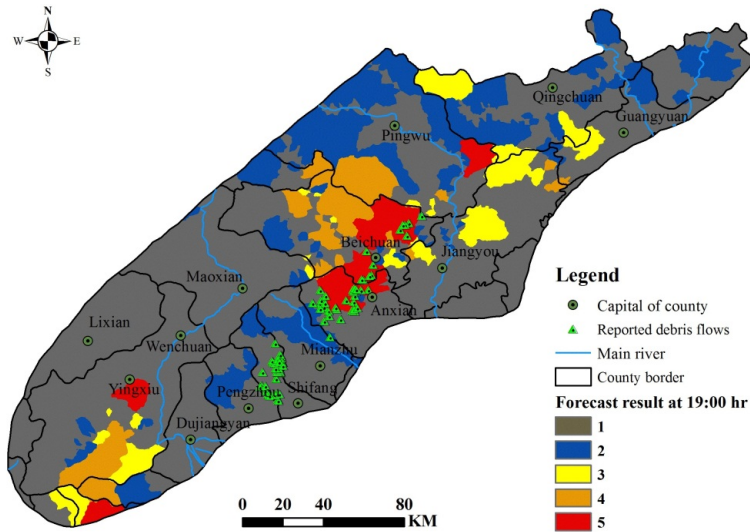


**Figure 13.** Transforming results by following the rule of highest warning level.

## Application and analysis of debris-flow early warning system in Wenchuan

D. L. Liu et al.

[Title Page](#)

[Abstract](#)

[Introduction](#)

[Conclusions](#)

[References](#)

[Tables](#)

[Figures](#)

[⏪](#)

[⏩](#)

[◀](#)

[▶](#)

[Back](#)

[Close](#)

[Full Screen / Esc](#)

[Printer-friendly Version](#)

[Interactive Discussion](#)



## Application and analysis of debris-flow early warning system in Wenchuan

D. L. Liu et al.

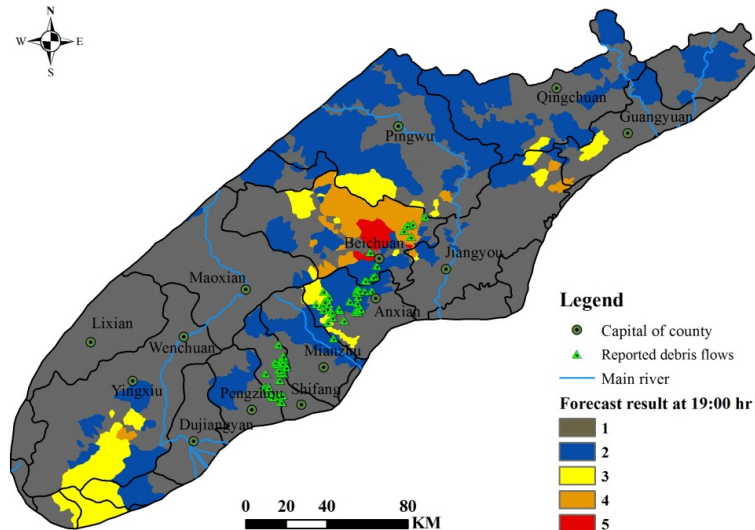


**Figure 14.** Transforming results by following the rule of most warning level.

[Title Page](#)

[Abstract](#)

[Introduction](#)

[Conclusions](#)

[References](#)

[Tables](#)

[Figures](#)

⏪

⏩

◀

▶

[Back](#)

[Close](#)

[Full Screen / Esc](#)

[Printer-friendly Version](#)

[Interactive Discussion](#)



## Application and analysis of debris-flow early warning system in Wenchuan

D. L. Liu et al.

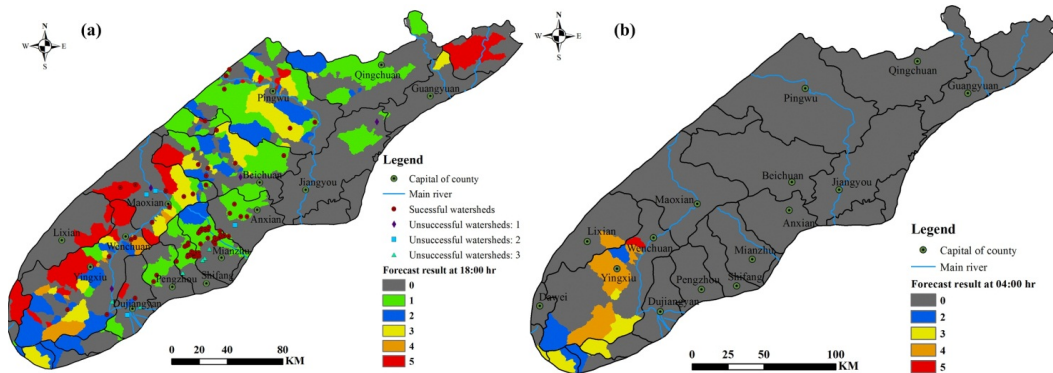


**Figure 15.** (a) Prediction results of the debris-flow prediction system based on the water–soil coupling mechanism at 18:00 (Beijing time zone) on 9 July 2013; (b) prediction results of the debris-flow prediction system based on the water–soil coupling mechanism at 04:00 (Beijing time zone) on 10 July 2014.

<a href="#">Title Page</a>	
<a href="#">Abstract</a>	<a href="#">Introduction</a>
<a href="#">Conclusions</a>	<a href="#">References</a>
<a href="#">Tables</a>	<a href="#">Figures</a>
<a href="#">⏪</a>	<a href="#">⏩</a>
<a href="#">⏴</a>	<a href="#">⏵</a>
<a href="#">Back</a>	<a href="#">Close</a>
<a href="#">Full Screen / Esc</a>	
<a href="#">Printer-friendly Version</a>	
<a href="#">Interactive Discussion</a>	

